Trans. Mo. Acad. Sci. **16**, 85 (1982); G. E. Gruell, *Northwest Sci.* **59**, 97 (1985); E. M. Steinauer and T. B. Bragg, *Am. Midl. Nat.* **118**, 358 (1987); T. W. Swetnam, *Science* **262**, 885 (1993); W. W. Covington and M. M. Moore, *J. For.* **92**, 39 (1994); B. E. Cutter and R. P. Guyette, *Am. Midl. Nat.* **132**, 393 (1994); P. Z. Fule, W. W. Covington, M. M. Moore, *Ecol. Appl.* **7**, 895 (1997)] resulted in an increased density of trees throughout the entire range of ponderosa pine forests (22×10^6 ha) [*Forest Type Groups of the United States* (USDA, Forest Service, Washington, DC, 1993), available at http://www.srsfia.usfs.msstate.edu/rpa/rpa93.htm] and an accumulation of 0.052 Pg C $year^{-1}$ over the past 90 years. These processes are well documented for individual sites, but their spatial extent is largely unknown. The calculated rates of carbon uptake are exaggerated and may be attributable more to changes in climate than to changes in management [T. W. Swetnam and J. L. Betancourt, *J. Clim.* **11**, 3128 (1998)].

23. M. L. Goulden, J. W. Munger, S. M. Fan, B. C. Daube, S. C. Wofsy, *Science* **271**, 1576 (1996).
24. *Forest Service Resource Inventories: An Overview* (USDA, Forest Service, Forest Inventory, Economics, and Recreation Research, Washington, DC, 1992).
25. It should be clear that we use the term "management" broadly. Much of the current sink attributed to management is a recovery from past use rather than a consequence of skillful environmental management.
26. Attributing growth to management, as opposed to environmental factors, is complicated because preindustrial rates of growth are not known. For our analysis, we obtained rates of growth from the literature (*17*), and, because most of the measurements were made after 1950, they may already include an enhanced rate of growth. If rates of growth have increased substantially over time, the emissions attributed to land-use change may have been underestimated in the early years of the analysis, whereas sinks may have been underestimated in recent decades.
27. H. Tian, J. M. Melillo, D. W. Kicklighter, A. D. McGuire, J. Helfrich, *Tellus*, in press.
28. P. Ciais *et al.*, *J. Geophys. Res.* **100**, 5051 (1995); R. F. Keeling, S. C. Piper, M. Heimann, *Nature* **381**, 218 (1996).
29. Land area of the United States is about 15% of the land area between 30° and 70°N.
30. D. W. Johnson, *Water Air Soil Pollut.* **64**, 83 (1992).
31. J. B. Gaudinski, S. E. Trumbore, E. A. Davidson, S. Zheng, *Biogeochemistry*, in press.
32. A. S. Donigian *et al.*, in *Advances in Soil Science. Soil Management and Greenhouse Effect*, R. Lal, J. Kimble, E. Levine, B. A. Stewart, Eds. (CRC Press, Boca Raton, FL,1995), pp. 121–135. Using the CENTURY model, these authors calculated that soil organic carbon increased over 60 to 70% of U.S. croplands, largely as a result of increased productivity between the years 1960 and 1990. They estimate that about 25% of the carbon initially lost through cultivation had been recovered.
33. P. Smith, D. S. Powlson, M. J. Glendining, J. U. Smith, *Global Change Biol.* **4**, 679 (1998); R. Q. Cannell and J. D. Hawes, *Soil Tillage Res.* **30**, 245 (1994).
34. D. L. Gebhart, H. B. Johnson, H. S. Mayeux, H. W. Polley, *J. Soil Water Conserv.* **49**, 488 (1994).
35. R. F. Stallard, *Global Biogeochem. Cycles* **12**, 231 (1998).
36. G. Marland, R. J. Andres, T. A. Boden, C. Johnston, A. Brenkert, Global, regional, and national CO_2 emission estimates from fossil fuel burning, cement production, and gas flaring: 1751–1996 (revised March 1999; 1950–1996 estimates are preliminary), available at http://cdiac.esd.ornl.gov/ndps/ndp030.html.
37. We reduced the carbon sink in forests estimated in (*2*) to account for the net effect of wood products. Birdsey and Heath (*2*) reported an accumulation of 0.027 Pg C $year^{-1}$ in new wood products and emissions of 0.099 Pg C $year^{-1}$ from oxidation of products, for a net release of 0.072 Pg C $year^{-1}$. Turner *et al.* (*3*) reported 0.124 Pg C $year^{-1}$ removed from the forest. Assuming the same distribution of these removals as in (*2*), we calculated that 0.097 Pg C was released and 0.027 Pg C was stored in long-lasting products, thus increasing the reported net sink by 0.027 Pg C $year^{-1}$.
38. Soil carbon is not measured in forest inventories. Turner *et al.* (*3*) assumed soils to be in balance (net flux = 0); Birdsey and Heath (*2*) assumed that soils accumulated carbon in proportion to growth in aboveground biomass.

39. We are grateful to two anonymous reviewers whose comments helped improve the precision and clarity of the paper. Research was supported through the Joint Program on Terrestrial Ecology and Global Change, grant number NAGW-4748 from the Terrestrial Ecology Program in NASA's Office of Earth Science.

19 March 1999; accepted 8 June 1999

An Adhesin of the Yeast Pathogen *Candida glabrata* Mediating Adherence to Human Epithelial Cells

Brendan P. Cormack,[1]*† Nafisa Ghori,[1] Stanley Falkow[1,2]

Candida glabrata is an important fungal pathogen of humans that is responsible for about 15 percent of mucosal and systemic candidiasis. *Candida glabrata* adhered avidly to human epithelial cells in culture. By means of a genetic approach and a strategy allowing parallel screening of mutants, it was possible to clone a lectin from a *Candida* species. Deletion of this adhesin reduced adherence of *C. glabrata* to human epithelial cells by 95 percent. The adhesin, encoded by the *EPA1* gene, is likely a glucan–cross-linked cell-wall protein and binds to host-cell carbohydrate, specifically recognizing asialo-lactosyl–containing carbohydrates.

Candida species are responsible for more than 8% of all hospital-acquired infections (*1*); the two most frequently encountered species are *C. glabrata* and *C. albicans* (*2*). *Candida albicans* is asexual and diploid, which complicates genetic analysis in this organism because both copies of a gene must be knocked out to uncover a recessive phenotype. Analysis of virulence in *C. albicans* has, therefore, been limited largely to reverse genetic approaches in which both copies of individual cloned genes are deleted and the resulting phenotype is assessed. *Candida glabrata*, although asexual, is haploid (*3*), which facilitates genetic analysis. In *C. glabrata*, it is possible to generate random mutants and screen for phenotypes of interest (*4*). Here, we demonstrate that this forward genetic approach can be used to analyze the host-pathogen interaction in *C. glabrata* and use this approach to identify an adhesin mediating adherence of *C. glabrata* to host epithelial cells.

The adherence of *Candida* to host cells has been the subject of intense investigation, and in the case of *C. albicans*, the yeast expresses a number of adhesins capable of interacting with a variety of ligands, including proteins [reviewed in (*5*)] and carbohydrates (*5–8*). Recently, it has also been shown that Hwp1p, a hypha-specific protein, is a substrate for mammalian transglutaminases and mediates covalent attachment of *C. albicans* to human buccal epithelial cells (*9*).

We found that *C. glabrata* adheres strongly to human epithelial cells in culture. In our assay (*10*), with a multiplicity of infection (MOI) of 1:1, between 10 and 20% of added yeast adheres to a monolayer of the human laryngeal carcinoma cell line HEp2 compared with 0.1% of added yeast for *Saccharomyces cerevisiae* (*11*). Scanning electron micrographs of *C. glabrata* bound to the surface of the monolayer show a marked and intimate interaction between the epithelial cell filopodia and the yeast cell (Fig. 1) (*12*). In transmission electron micrographs (*13*), a similar tight association is seen between the surface of the yeast cell and the surface of the epithelial cell, suggesting that the host ligand is broadly distributed on these tissue culture cells. This interaction is dependent on Ca^{2+} because adherent yeast can be removed with EGTA or with EGTA titrated with Mg^{2+} but not with EGTA titrated with Ca^{2+} (*13*).

To identify the yeast gene mediating the interaction of *C. glabrata* with epithelial cells, we undertook a mutant screen. We implemented a number of genetic tools to facilitate this analysis. First, we used a *ura3* deletion strain congenic with a virulent clinical isolate (*4*). Second, we used a variation

[1]Department of Microbiology and Immunology, Stanford University School of Medicine, Fairchild D039, 299 Campus Drive, Stanford, CA 94305–5124, USA. [2]Protein Design Labs, 34801 Campus Drive, Fremont, CA 94555, USA.

*Present address: Johns Hopkins Medical Institute, Department of Molecular Biology and Genetics, 725 N. Wolfe Street, Baltimore, MD 21205, USA.

†To whom correspondence should be addressed. E-mail: bcormack@jhmi.edu

of signature-tagged mutagenesis (*14*), a strategy permitting parallel screening of multiple mutants in a single complex pool of mutants. In this strategy, each mutant in a pool of mutants also carries a unique sequence tag flanked by constant polymerase chain reaction (PCR) priming sites that permit the amplification of all the tags in a pool in a single PCR amplification. The fate of individual mutants is mirrored by the fate of their cognate oligonucleotide tags and is followed by means of hybridization to a membrane on which all the tags have been arrayed. We generated 96 strains of *C. glabrata* by integrating 96 different sequence tags in the already disrupted *URA3* locus (*15*). In control experiments, differences of twofold to threefold in representation were easily detected (*13*). Finally, we used a method of insertional mutagenesis that was based on our observation that *C. glabrata* had a very efficient system of nonhomologous integration. These insertions were randomly distributed at the genome level and gave rise to auxotrophs at a frequency of 0.25% (*4*).

To generate a mutant library, we transformed each of the 96 strains with linearized YipLac211 [a plasmid carrying the *S. cerevisiae URA3* gene (*16*)] and isolated 100 Ura^+ transformants for each of the 96 tagged strains. This collection of 9600 mutants was assembled into 100 pools of 96 in which each pool consisted of a complete set of the 96 tagged strains.

Pools of mutants were allowed to adhere to duplicate monolayers of human cultured epithelial cells (HEp2 cells) in a standard adherence assay (*10*). The adherent yeast and the input pool were recovered and grown on yeast extract, peptone, and dextrose (YPD) plates overnight. Genomic DNA was prepared from the yeast in the input and two adherent output pools, and the sequence tags were amplified by PCR. The amplified tags were labeled with [α-^{32}P]deoxycytidine triphosphate and were used to hybridize to triplicate membranes on which all 96 tags were immobilized. The filters were analyzed with a phosphorimager, and nonadherent mutants were detected by the presence of the cognate tag in the input pool and its absence in the output pools (Fig. 2A). We screened 50 pools comprising 4800 mutants and isolated 31 mutants that were altered in their adherence to HEp2 cells. Among these mutants, five were hyperadherent (*13*) and 16 were totally nonadherent (Fig. 2B and Fig. 2A, strain g6). For 10 mutants, adherence was reduced but not eliminated (*13*).

To identify the loci disrupted in the nonadherent mutants, we cloned the DNA flanking the Yiplac211 insertions. Genomic DNA for each mutant strain was digested with Eco R1 (which does not digest in the Yiplac211 plasmid sequence), circularized with ligase,

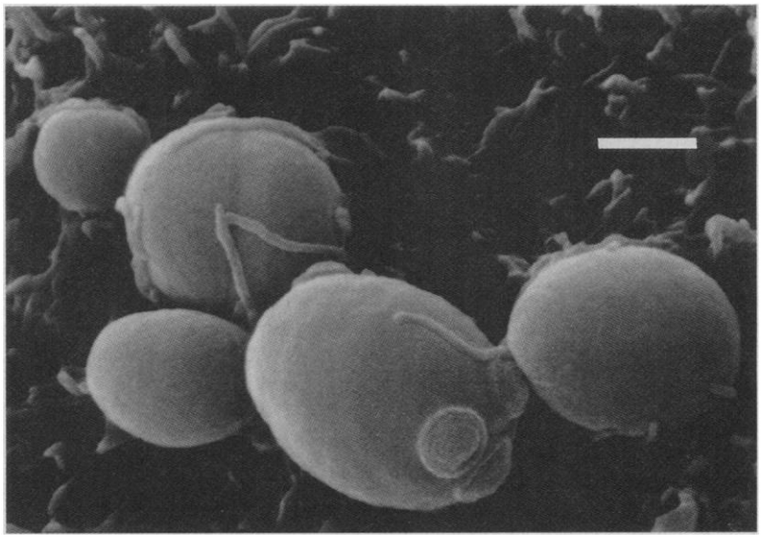

Fig. 1. Scanning electron micrograph (*12*) of *C. glabrata* adhering to cultured HEp2 cells. Scale bar, 1 μM.

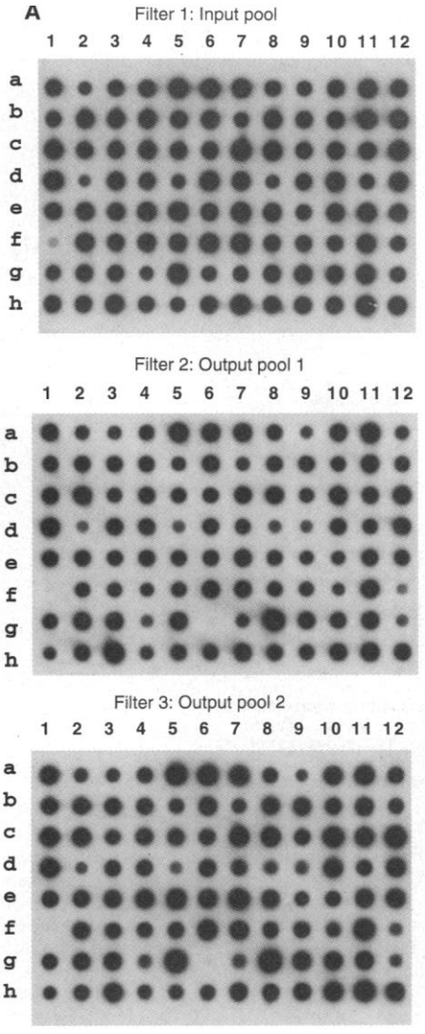

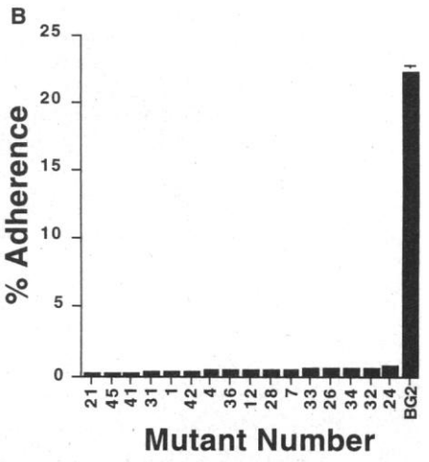

Fig. 2. (**A**) Signature tag representation in input and recovered adherent output populations of *C. glabrata* mutant pool 15. Triplicate filters with identical sets of 96 immobilized signature tags. Each filter was probed with labeled PCR product derived from amplification of the tags present in a population of yeast cells. Filter 1, input population of cells after overnight growth in YPD. Filter 2, population adherent to HEp2 cells. Filter 3, population adherent to HEp2 cells in duplicate adherence assay. (**B**) Adherence of *C. glabrata* mutants. Individual mutants were reconstructed in parent strain and tested in the standard adherence assay (*10*) *Candida glabrata* strain BG2 is the wild-type parent of all of the mutants. The assays were carried out in triplicate.

and transformed into *Escherichia coli*. This resulted in recovery of a plasmid consisting of Yiplac211 and the genomic DNA flanking the original insertion site. When we reintroduced the Yiplac211 plasmid into the original site of insertion in the parental strain (*17*), the regenerated mutants were also nonadherent, demonstrating that the insertion was responsible for the mutant phenotype. Sequence analysis of the DNA flanking the insertion site for 16 nonadherent mutants revealed that 14 of the 16 insertion mutants were in the same 1.4-kb locus (Fig. 3A). These insertions were in the noncoding region upstream of a large open reading frame (ORF), reflecting the fact that illegitimate recombinants in *C. glabrata* are directed almost exclusively to noncoding regions (*4*). The sequence of the gene downstream of these 14 insertions revealed an ORF encoding a 1034–amino acid protein (*18*). We have named this gene *EPA1*, for Epithelial Adhesin 1. Deletion of the coding region of *EPA1* rendered the yeast nonadherent (Table 1). Restoration of the *EPA1* gene, either on a plasmid or by integration at the natural *EPA1* locus, restored adherence, showing that the nonadherent phenotype of the *epa1*-null strain is due to loss of *EPA1* (Table 1).

Expression of *EPA1* in *S. cerevisiae* permitted *S. cerevisiae* to adhere as well as *C. glabrata* to epithelial cells (Table 1). Thus, *EPA1* was sufficient to mediate adherence in the context of the *S. cerevisiae* cell. In its domain structure (Fig. 3B), this protein is a member of a large family of cell-wall proteins in yeast. Amino acids 6 to 24 (12 of 19 hydrophobic) are a consensus signal sequence, and the hydrophobic amino acids 1020 to 1033 at the COOH-terminus are a consensus hydrophobic signal for addition of a glycosyl-phosphatidylinositol (GPI) anchor. Asn^{1011}, which is followed by two small amino acids Ala^{1012} and Ile^{1013}, is the likely addition point for the GPI anchor. The COOH-terminal two-thirds of the protein (approximately amino acids 331 to 944) is highly enriched for serine and threonine (43.8%); between amino acids 580 and 700 are three direct repeats of the 40–amino acid motif shown in Fig. 3C. The NH_2-terminal domain has slight homology with the *S. cerevisiae* flocculin *FLO1*, a Ca^{2+}-dependent lectin (Fig. 3D).

As deletion of the *EPA1* gene reduced adherence by 95%, we conclude that overall adherence of wild-type *C. glabrata* in our assay is largely a reflection of *EPA1*-mediated binding. We characterized the host ligand requirements for *EPA1* binding. As mentioned above, adherence of *C. glabrata* to epithelial cells required Ca^{2+}. Binding of *C. glabrata* to epithelial cells was totally inhibited by 10 mM galactose or lactose but not by 10 mM sialyl-lactose or 100 mM of a number of other sugars or by solutions (1 mg/ml) of various glycoconjugates (Table 2). The concentration at which lactose or *N*-acetyl lactosamine (LacNAc) inhibited 50% of *C. glabrata* binding to epithelial cells was 1.25 to 1.5 mM, consistent with LacNAc being closely related to the natural ligand. Adherence of *S. cerevisiae* cells expressing *EPA1* was also dependent on Ca^{2+} and was 50% inhibited by 1.5 mM lactose (*13*), suggesting that *EPA1* function in *S. cerevisiae* closely

Table 1. *EPA1* mediates adherence of yeast cells to epithelial cells. *Candida glabrata* strain: BG2 (*4*). *Candida glabrata epa1Δ*: BG176 and BG178, two independent deletions of the *EPA1* coding region. *EPA1* restored: BG184 and BG186, independent restorations of the *EPA1* genomic locus in deletion strains BG176 and BG178 with a two-step replacement strategy (*31*). *Saccharomyces cerevisiae*: strain BY4741 (*MATa ura3Δ0 leu2Δ0 his3Δ0, LYS2 met15Δ0*). *Saccharomyces cerevisiae* + p*EPA1*: BY4741 transformed with p*EPA1* (*36*). Data shown are for adherence to the CHO-derived epithelial cell line Lec2. Essentially identical results were obtained for adherence to HEp2 cells. All strains were tested in triplicate.

Strain	Adherence (%)
C. glabrata	100 ± 16
C. glabrata epa1Δ	2.1 ± 1.2
C. glabrata EPA1 (restored)	86 ± 16
S. cerevisiae	1.8 ± 0.9
S. cerevisiae + p*EPA1*	99 ± 14

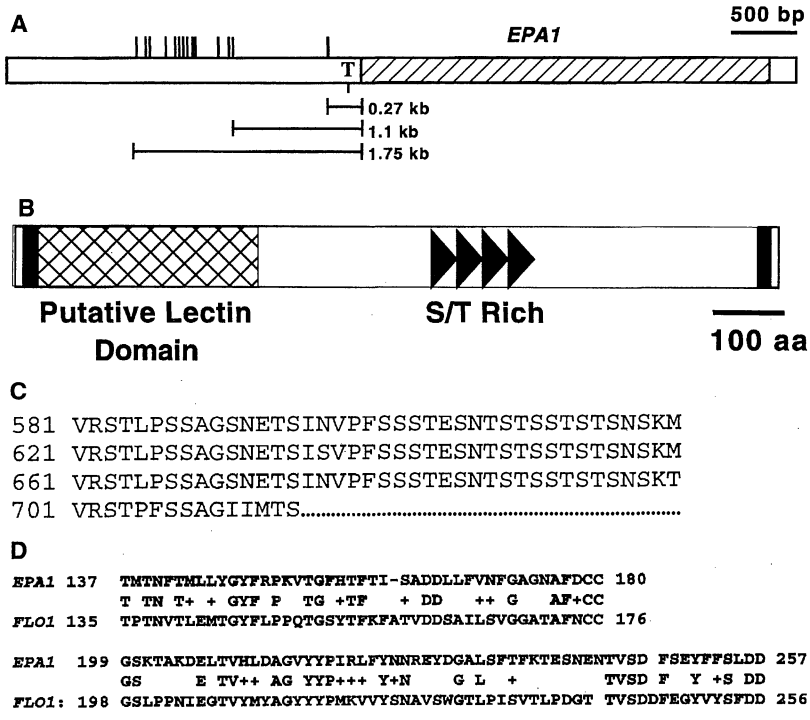

Fig. 3. (**A**) Physical map of 14 insertions at the *EPA1* locus. Insertion sites are marked with vertical hatch marks. The ORF is shown as a hatched box. A "T" marks a consensus TATA box. bp, base pairs. (**B**) Structure of the *EPA1* protein. Filled black boxes are hydrophobic stretches. The open box is highly enriched for Ser (S) and Thr (T); the hatched box has slight homology to *FLO1* from *S. cerevisiae* (*34, 35*). aa, amino acid. (**C**) The direct repeat region of *EPA1*. (**D**) Alignment of amino acid sequence of *EPA1* and *FLO1*. Single-letter abbreviations for the amino acid residues are as follows: A, Ala; C, Cys; D, Asp; E, Glu; F, Phe; G, Gly; H, His; I, Ile; K, Lys; L, Leu; M, Met; N, Asn; P, Pro; Q, Gln; R, Arg; S, Ser; T, Thr; V, Val; W, Trp; and Y, Tyr.

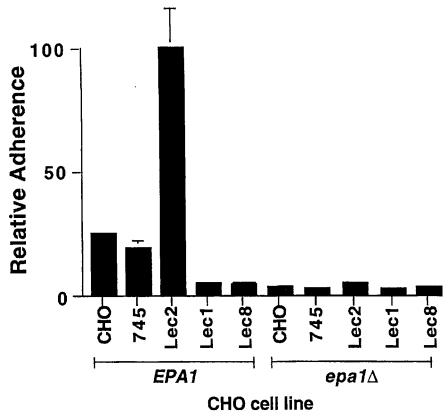

Fig. 4. Adherence (in percent) of *Candida* species to cultured CHO cells. Adherence (*10, 20*) of *C. glabrata* strains BG2 (*EPA1*) and BG178 (*epa1Δ*) to CHO cells and derivative glycosylation-deficient CHO cells. The strains are CHO (ATCC CRL-1781); 745 GAG deficient: pgsA745(ATCC CRL-2242); Lec2 sialic acid deficient (ATCC CRL-1736); Lec1 GlcNAc deficient (ATCC CRL-1735); and Lec8 galactose deficient (ATCC CRL-1737). All experiments were performed in triplicate.

mirrors its function in *C. glabrata*.

These data suggested either that *EPA1*, like *FLO1*, is a Ca^{2+}-dependent lectin or that *EPA1* encodes a glycoprotein whose carbohydrate modifications are recognized by a host lectin. To distinguish between these possibilities, we determined whether adherence was affected by treatment with sodium periodate (NaI), which cleaves sugar rings (*19*). Adherence was eliminated by pretreatment of the HEp2 cell with NaI, whereas treatment of the yeast cell with NaI did not affect adherence (*13*). This is consistent with *EPA1* being a lectin and the host ligand being carbohydrate. To further characterize host requirements for binding by *EPA1*, we analyzed binding (*20*) of *C. glabrata* to chinese hamster ovary (CHO) epithelial cells and to a number of glycosylation-deficient CHO derivative lines (*21*). *Candida glabrata* was as adherent to CHO cells or to the glycosaminoglycan (GAG)–deficient line pgsA745 as to HEp2 cells. By contrast, binding to the sialic acid–deficient line Lec2 was increased by fivefold to 10-fold (Fig. 4). In Lec2 cells, the terminal glycosylation of complex N-linked carbohydrates is *N*-acetyl lactosamine (Galβ1-4 GlcNAc). In cells with reduced levels of surface Gal or GlcNAc (Lec1 and Lec8), binding of *C. glabrata* was reduced to background levels, equivalent to binding by the *epa1*-null strain.

We compared the virulence of the *EPA1* and *epa1*Δ strains in two murine models of mucosal infection (*22*). In vaginal or gastrointestinal (GI) tract infections (*23*) with an inoculum of between 10^6 and 10^8 *C. glabrata*, we could find no difference between *EPA1* and *epa1*Δ strains in initial colonization or subsequent persistence (*13*). In infections of animals with a mixture of oligo-tagged *EPA1* and *epa1*Δ strains, there was no detectable difference in the tag representation (and by extension the yeast strains) either immediately after colonization (days 1 to 2) or in persistently infected animals (days 9 to 15) (*13*).

Table 2. Inhibition of adherence of *C. glabrata* to HEp2 cells by saccharides. The concentration of glyconjugate at which adherence is 50% of adherence in the absence of glycoconjugate is given. NANA, *N*-acetyl neuraminic acid (sialic acid); GlcNAc, *N*-acetyl glucosamine; GalNAc, *N*-acetyl galactosamine.

Glycoconjugate	[50% inhibition]
Glucose	>200 mM
Galactose	10 mM
Fucose	>200 mM
Xylose	>200 mM
Mannose	>200 mM
Lactose	1.5 mM
LacNAc	1.25 mM
Sialyl-LacNAc	>10 mM
NANA	>200 mM
GlcNAc	>200 mM
GalNAc	>200 mM
Methyl-D pyranoside	>200 mM
Mannosamine	>200 mM
Dextran	>1 mg/ml
Dextran-SO_4	>1 mg/ml
Mannan	>1 mg/ml
Hyaluronic acid	>1 mg/ml
Heparin	>1 mg/ml
Albumin	>1 mg/ml
Fucoidan	>1 mg/ml
Fetuin	>1 mg/ml
Asialofetuin	>1 mg/ml
Chondroitin-SO_4-A	>1 mg/ml
Chondroitin-SO_4-B	>1 mg/ml
Chondroitin-SO_4-C	>1 mg/ml

Our data show that *EPA1* is required for efficient in vitro adherence to human epithelial cells in culture. Elimination of its function reduced in vitro adherence by 20-fold. *EPA1*-mediated adherence was inhibited by lactose and *N*-acetyl-lactosamine, but not by sialyllactose. Furthermore, adherence was markedly increased by reduction of surface sialylation, consistent with recognition of an asialo-lactosyl-glycoconjugate. The ligand specificity for *EPA1* is related to the specificity of a number of different *Candida* and fungal lectins. Specifically, Krivan's group has shown that phylogenetically diverse fungi express a lectin specific for lactosyl ceramide (Galβ1-4Glcβ1-1Ceramide) (*7*). Irvin's group has shown that stationary phase *C. albicans* expresses a lectin activity that preferentially binds to asialo-GM1 (gangliotetraosylceramide: Galβ13GalNAcβ1-4Galβ1-4Glcβ1-1Ceramide) (*6*, *24*). Cameron and Douglas have shown that stationary phase *C. albicans* expresses a lectin activity that likely binds to the type 2 H blood group antigen (Fucα1-2)Galβ1-4GlcNAc (*25*). These three carbohydrate ligands share common features with the ligand for Epa1p, having as their core component Galβ1-4 GlcNAc or Galβ1-4 Glc, both of which are good ligands for Epa1p. This potential conservation in ligand specificity may point to homologous adhesins in *C. albicans* and other pathogenic fungi. Alternatively, it may reflect convergent evolution of lectin activities specific for conserved glycoconjugates on the mammalian epithelial cell surface.

A number of adhesins have been described in *C. albicans* that contribute to overall adherence [reviewed in (*5*)]. Four genes mediating adherence of *C. albicans* to unknown ligands on human cultured cells have been cloned (*9*, *26*), although their relative contribution to adherence is unknown. A similar redundancy of adhesins probably exists in *C. glabrata* and might explain why the *EPA1*-null mutant shows no phenotype in vivo especially given that this adhesin is responsible for 95% of in vitro adherence. Alternatively, a high-affinity ligand present on HEp2 cells and CHO cells may not be present on the tissues colonized in the models we examined. A more complete description of the total adhesin complement of *C. glabrata*, as well as *C. albicans*, will be a first step in understanding the role of adherence in host colonization and persistence.

References and Notes

1. D. R. Schaberg, D. H. Culver, R. P. Gaynes, *Am. J. Med.* **91**, 72S (1991).
2. P. Schuman *et al.*, *Clin. Infect. Dis.* **27**, 1161 (1998); M. A. Pfaller *et al.*, *Diagn. Microbiol. Infect. Dis.* **33**, 217 (1999); M. A. Pfaller, R. N. Jones, S. A. Messer, M. B. Edmond, R. P. Wenzel, *ibid.* **30**, 121 (1998); M. A. Pfaller *et al.*, *ibid.* **31**, 289 (1998); M. H. Nguyen *et al.*, *Am. J. Med.* **100**, 617 (1996).
3. W. L. Whelan, *Crit. Rev. Microbiol.* **14**, 99 (1987).
4. B. P. Cormack and S. Falkow, *Genetics* **151**, 979 (1999).
5. M. K. Hostetter, *Clin. Microbiol. Rev.* **7**, 29 (1994); M. L. Pendrak and S. A. Klotz, *FEMS Microbiol. Lett.* **129**, 103 (1995); R. A. Calderone, *Arch. Med. Res.* **24**, 275 (1993).
6. L. Yu, K. K. Lee, R. S. Hodges, W. Paranchych, R. T. Irvin, *Infect. Immun.* **62**, 5213 (1994).
7. V. Jimenez-Lucho, V. Ginsburg, H. C. Krivan, *ibid.* **58**, 2085 (1990).
8. F. D. Tosh and L. J. Douglas, *ibid.* **60**, 4734 (1992); I. A. Critchley and L. J. Douglas, *J. Gen. Microbiol.* **133**, 637 (1987).
9. J. F. Staab, S. D. Bradway, P. L. Fidel, P. Sundstrom, *Science* **283**, 1535 (1999).
10. In our adherence assay, epithelial cells HEp2 (ATCC CCL23) cells were grown in RPMI media supplemented with 10% fetal bovine serum (FBS) and washed twice with phosphate-buffered saline (PBS) and resuspended in RPMI without serum. *Candida glabrata* strains were grown overnight to stationary phase at 30°C in YPD media. They were diluted into fresh media and grown in logarithmic phase for 2 to 4 hours. Each culture was then was added at the stated MOI. Contact between the HEp2 cells and the yeast cells was initiated by brief (1 to 2 min) centrifugation (500*g*). After incubation for 1 hour, nonadherent cells were removed by four to five washes in PBS. Care was taken that the monolayer remained intact during these washes. Adherent cells were recovered by lysis of the monolayer in 0.1% Triton X-100 and quantified by overnight growth on YPD plates. Percentage of adherent cells was calculated as colony-forming units (CFUs) recovered by lysis of the monolayer divided by CFUs added. Alternatively, yeast cells were labeled by overnight growth in YPD with [^{35}S]methionine, washed extensively in PBS to remove unincorporated label, and then diluted into fresh media as before. Adherence was calculated as the percentage of input counts per minute that were recovered by lysis of the monolayer after the washing step. Yeast media were prepared as described (*27*).
11. Adherence was measured for *C. albicans* strain 5314 (*28*), *C. glabrata* strain BG2 (*4*), and *S. cerevisiae* strains YJM263, YJM128, YJM309, YJM210, and YJM436 (*29*). All except YJM263 are clinical isolates.
12. Adherence assays were carried out as usual, and the monolayer with adherent yeast was fixed in PBS with 2% paraformaldeyde. The monolayer with associated yeast was cut out of the microtiter dish and prepared for electron microscopy as described (*30*). In control experiments, yeast deleted for the *EPA1* gene was not found to be associated with the HEp2 monolayer by microscopy.
13. B. P. Cormack and S. Falkow, data not shown.
14. M. Hensel *et al.*, *Science* **269**, 400 (1995).
15. The oligonucleotide sequence tags were similar to those used by Hensel *et al.* (*14*). The sequence tags had Sal 1 restriction sites at the termini. The overall sequence was GTCGACATCCTACAACCTCTCTAGA(N_{40})TCTAGAGGTTAGAATGGGTAGTCGAC. We screened 300 tags for a subset of 96 that hybridized well and did not cross hybridize with one another. Using a standard two-step disruption (*31*), we introduced these 96 tags into the *C. glabrata* genome as Sal I fragments into the Xho 1 site of the *neo* gene that had been used to disrupt the *URA3* gene of *C. glabrata* (*4*). To verify that the manipulations required for tagging did not compromise the strains for growth, we pooled the 96 strains and grew them for 40 generations in minimal media (1/1000 serial dilutions, grown to saturation and repeated four times). Analysis of the tag representation in the initial pool of strains and in the pool after 40 generations showed that the representation of the 96 strains at the beginning and end was essentially

identical. Thus, there is a less than 2% difference in doubling time between all 96 strains. The primers used for amplification of the tags were ATCCTACAACCTCTCTAG and TACCCATTCTAACCTCTA.
16. R. D. Gietz and A. Sugino, *Gene* **74**, 527 (1988).
17. To regenerate the mutant, we digested the plasmids with Eco R1 and used them to transform strain BG14. The genomic DNA flanking YipLac211 directed homologous recombination back to the original locus, thus regenerating the original insertion mutant.
18. The *EPA1* sequence has been deposited in GenBank (accession number AF149048)
19. Hep2 monolayers were fixed with 2% paraformaldehyde. Surface carbohydrates were disrupted by incubation in the dark at room temperature with 10 mM sodium metaperiodate in 50 mM sodium acetate (pH 4.5) for 1 hour. Monolayers were washed twice in PBS and reduced with 50 mM sodium borohydride (50 mM in PBS) for 30 min at room temperature. Monolayers were rinsed with PBS and used in adherence assays. Control monolayers were treated identically with the exception of the sodium metaperiodate. Yeast cells treated with periodate were not fixed, and washes were carried out in microcentrifuge tubes with centrifugation at 500*g* (*32*).
20. CHO cells and their derivatives were cultured in α-MEM with 10% FBS. The adherence assays were carried out identically to those with HEp2 cells.
21. P. Stanley and L. Siminovitch, *Somatic Cell Genet.* **3**, 391 (1977); P. Stanley, *Mol. Cell. Biol.* **1**, 687 (1981).
22. P. L. Fidel Jr., J. L. Cutright, L. Tait, J. D. Sobel, *J. Infect. Dis.* **173**, 425 (1996).
23. The vaginal candidiasis model we used is a modification of one described for *C. glabrata* in the literature (*22*). In our modification, we administered two doses of estrogen, one 5 days and one 3 days before infection. These doses increase the overall CFUs recoverable to 10^5 to 10^6 per animal at day 6 and decreases mouse-to-mouse variability in colonization. Subsequent to these initial doses of estrogen, no more is administered. The GI infection model is a colonization model in which 6- to 7-week-old DBA2 mice are given 10^8 organisms by oral inoculation. By day 3, the most substantial site of colonization in the GI tract was the stomach, consistent with what is seen in *C. albicans* infections. About 1 to 5×10^4 CFUs persisted at this site for 9 days. By day 15 after infection, the recoverable CFUs had dropped to about 10^3 per animal.
24. L. Yu *et al.*, *Infect. Immun.* **62**, 2843 (1994).
25. B. J. Cameron and L. J. Douglas, *ibid.* **64**, 891 (1996).
26. Y. Fu *et al.*, *ibid.* **66**, 1783 (1998); N. K. Gaur and S. A. Klotz, *ibid.* **65**, 5289 (1997); C. A. Gale *et al.*, *Science* **279**, 1355 (1998).
27. F. Sherman, G. R. Fink, J. B. Hicks, *Methods in Yeast Genetics* (Cold Spring Harbor Laboratory, Cold Spring Harbor, NY, 1986).
28. W. A. Fonzi and M. Y. Irwin, *Genetics* **134**, 717 (1993).
29. K. V. Clemons, J. H. McCusker, R. W. Davis, D. A. Stevens, *J. Infect. Dis.* **169**, 859 (1994).
30. L. Pascopella *et al.*, *Infect. Immun.* **63**, 4329 (1995).
31. K. Struhl, *Nature* **305**, 391 (1983).
32. J. W. St. Geme III, *Infect. Immun.* **62**, 3881 (1994).
33. D. Mumberg, R. Muller, M. Funk, *Gene* **156**, 119 (1995).
34. J. Watari *et al.*, *Yeast* **10**, 211 (1994).
35. A. W. Teunissen, E. Holub, J. van der Hucht, J. A. van den Berg, H. Y. Steensma, *ibid.* **9**, 423 (1993).
36. pEPA1 was made by cloning the Hind III—Eco RI fragment of *EPA1* [which includes the coding region and 3′ untranslated region as well as 54 nucleotides upstream of the ATG] into the *S. cerevisiae* expression vector p416TEF (*33*). Adherence of two independent transformants was tested in triplicate.
37. We thank P. Fidel and J. Sobel for the gift of the *C. glabrata* clinical isolate; K. Clemons and D. Stevens for the clinical *S. cerevisiae* isolates; E. Ortega-Barria for many helpful discussions and advice; and J. Mecsas, C. Greider, and S. Fisher for a critical reading of the manuscript. This work was funded by a grant to S.F. from SmithKline Beecham. B.P.C. was supported by a postdoctoral fellowship from the Helen Hay Whitney Foundation and a career award from the Burroughs Wellcome Fund.

9 March 1999; accepted 18 May 1999

Transcriptional Activation of APETALA1 by LEAFY

Doris Wagner, Robert W. M. Sablowski,* Elliot M. Meyerowitz†

Plants produce new appendages reiteratively from groups of stem cells called shoot apical meristems. LEAFY (LFY) and APETALA1 (AP1) are pivotal for the switch to the reproductive phase, where instead of leaves the shoot apical meristem produces flowers. Use of steroid-inducible activation of LFY demonstrated that early expression of *AP1* is a result of transcriptional induction by LFY. This *AP1* induction is independent of protein synthesis and occurs specifically in the tissues and at the developmental stage in which floral fate is assumed. Later expression of *AP1* appears to be only indirectly affected by LFY.

The above ground body plan in higher plants is generated postembryonically by a group of undifferentiated stem cells, the shoot apical meristem (SAM). Initially, the *Arabidopsis thaliana* SAM produces leaves with axillary, second-order shoot meristems. At the transition to the reproductive phase, the primary shoot switches to the production of flowers. Two meristem identity factors, LEAFY (LFY) and APETALA1 (AP1), are necessary and sufficient for this transition (*1*–*4*). Severe disruption of the onset of reproduction is observed in the loss-of-function *lfy-6* mutant; most flowers are replaced by leaves and second-order shoots (*3*). In the strong *ap1-1* mutant, flowers have partial shoot character (*1*). The gain-of-function phenotype produced by constitutive expression of either LFY or AP1 results in formation of flowers or leaves and flowers in positions normally occupied by leaves and second-order meristems (*2*, *4*). The LFY protein localizes to the nucleus, and LFY binds to a putative *AP1* promoter element in vitro (*5*). AP1 is a potential transcriptional target of LFY because it acts, in part, downstream of LFY (*1*–*7*). Moreover, *AP1* expression is delayed and reduced in *lfy* mutants [our data and (*2*, *8*–*10*)], whereas constitutive ectopic expression of LFY results in precocious *AP1* expression (*5*). However, these data do not allow separation of direct transcriptional activation by LFY from downstream effects that influence gene expression. To test whether LFY acts as a transcriptional activator in vivo, we constructed a steroid hormone–inducible, posttranslational LFY switch (*11*). This switch allows us to monitor the immediate effect of LFY activation on transcription, in the presence of translational inhibitors.

We transformed plants segregating for the sterile *lfy-6*–null mutation with a constitutively expressed translational fusion of LFY to the rat glucocorticoid receptor hormone binding domain [35S::LFY-GR (*12*)]. Using antiserum to LFY (*13*), we identified several lines expressing full-length fusion protein (Fig. 1A). The amount of LFY-GR protein detected in the nuclei increased after dexamethasone hormone treatment (*14*) (compare Fig. 1C with Fig. 1B). Thus, activation of the fusion protein results in proper subcellular localization of LFY-GR (Fig. 1D) (*5*, *15*).

In *lfy-6*–null mutants, floral organs that require the expression of the class B homeotic genes (petals and stamens) are absent (*3*, *16*). To test whether the fusion protein is biologically active, we followed the development of *lfy-6* 35S::LFY-GR flowers after dexamethasone treatment. As expected, petals and stamens were also absent in untreated *lfy-6* 35S::LFY-GR flowers (Fig. 1E). This defect was partially or fully rescued after hormone treatment (Fig. 1, F and G, respectively). In addition, hormone treatment of seedlings resulting from an outcross of *lfy-6* 35S::LFY-GR to the *Ler* wild type reproduced characteristic LFY gain-of-function phenotypes (*4*) in that second-order shoots were converted to flowers (Fig. 1, H and I). Similarly, treatment of *lfy-6* 35S::LFY-GR seedlings caused conversion of secondary shoots to flowers (*17*). These data demonstrate that the LFY switch we constructed is functional.

To test whether LFY acts as a transcriptional activator in vivo, we monitored *AP1* expression in *lfy-6* inflorescences after LFY-GR activation using in situ hybridization (*14*). Early *AP1* expression in the wild type is first observed in young stage 1 (*18*) flowers immediately after the transition to flowering (Fig. 2H) (*19*). By contrast, *AP1* is absent from stage 1 flowers in *lfy-6* inflorescences immediately after the transition to flowering (compare Fig. 2,

California Institute of Technology, Division of Biology 156-29, Pasadena, CA 91125, USA.

*Present address: Molecular Genetics Department, John Innes Centre, Norwich NR4 7UH, UK.
†To whom correspondence should be addressed. E-mail: meyerow@cco.caltech.edu